Applied Soft Computing 11 (2011) 5215–5229

Contents lists available at ScienceDirect

Applied Soft Computing

journal homepage: www.elsevier.com/locate/asoc

A high throughput system for intelligent watermarking of bi-tonal images

Eduardo Vellasques*, Robert Sabourin, Eric Granger

École de Technologie Supérieure, Université du Québec, Montreal, Canada

ARTICLE INFO

Article history:
Received 28 October 2010
Received in revised form 29 March 2011
Accepted 10 May 2011
Available online 23 May 2011

Evolutionary computing
Particle Swarm Optimization
Dynamic optimization
Digital watermarking
Intelligent watermarking

ABSTRACT

In intelligent watermarking of document images, evolutionary computing (EC) techniques are employed in order to determine embedding parameters of digital watermarking systems such that the trade-off between watermark robustness and image fidelity is optimized. However, existing techniques for intelligent watermarking rely on full optimization of embedding parameters for each image. This approach does not apply to high data rate applications due to its high computational complexity. In this paper, a novel intelligent watermarking technique based on Dynamic Particle Swarm Optimization (DPSO) is proposed. Intelligent watermarking of bi-tonal image streams is formulated as a dynamic optimization problem. This population-based technique allows to evolve a diversified set of solutions (i.e., embedding parameters) to an optimization problem, and solutions from previous optimizations are archived and re-considered prior to triggering new optimizations. In such case, costly optimization may be replaced by direct recall of quasi identical solutions. Simulations involving the intelligent watermarking of several long streams of homogeneous PDF document images resulted in a decrease of computational burden (number of fitness evaluations) of up to 97.2% with a negligible impact on accuracy.

1. Introduction

The digitalization, storage and transmission of document images play a vital role in many sectors, including government, health care and banking. Modern scanning devices have produced massive quantities of digitized documents, a situation that poses serious privacy threats, because most of these documents contain sensitive fiscal, medical and financial information. The enforcement of the confidentiality, integrity, and authenticity of these images has therefore become a very active research topic.

Cryptography has traditionally been employed as a mean of enforcing these aspects for different types of data. However, as pointed by Cox et al. [1], in conventional cryptographic systems, once the data is decrypted there is no way to track its reproduction or transmission. Digital watermarking, which is the practice of imperceptibly altering an image in order to embed a message about it [2] is a complement to cryptography and, can be employed in order to enforce the integrity and authenticity of document images. Although digital watermarking has been successfully employed in the protection of many different types of media such as audio, video and images [3], this paper will focus on the watermarking of long streams of bi-tonal document images with similar structure as bank cheques, for example. The three main properties of a digital watermarking system are the data payload or capacity (amount of information that can be embedded within an image), robustness (watermark resistance against intentional and unintentional image processing operations) and fidelity (similarity between original and watermarked images). A gain in one of these properties usually comes at the expense of a loss in others.

Each application has a different requirement with regard to payload, fidelity and robustness. A common approach is to employ Constant Embedding Rate (CER) to set the payload, and to find an optimal trade-off for the other two properties. A watermark that is robust enough to resist attacks is embedded (as long as these attacks do not affect the commercial value of the watermarked image), without introducing visual artifacts. Some watermarking systems allow embedding multiple watermarks with different robustness levels [4]. A robust watermark is usually employed in the enforcement of authenticity since it can survive some attacks while a fragile one is easily destroyed by tampering and can be employed in the enforcement of integrity.

Finding the optimal trade-off between fidelity and robustness is a very challenging problem because the payload varies for different types of images. In intelligent watermarking [5], evolutionary computing (EC) techniques such as Genetic Algorithms (GAs) [6] and Particle Swarm Optimization (PSO) [7] have been proposed to determine the optimal embedding parameters for each specific image. The basic principle is to evolve a population of potential embedding parameters through time using a mix of robustness and quality metrics as objective function [8–17]. Genetic programming has also been proposed in a similar context [18]. Such EC-based

* Corresponding author. Tel.: +1 514 396 8800x7675.
E-mail addresses: evellasques@livia.etsmtl.ca (E. Vellasques), robert.sabourin@etsmtl.ca (R. Sabourin), eric.granger@etsmtl.ca (E. Granger).

1568-4946/$ – see front matter © 2011 Elsevier B.V. All rights reserved.
doi:10.1016/j.asoc.2011.05.038

approaches are not feasible in high data rate applications because of their high computational cost [10], mainly because the optimization of a single image may require hundreds of thousands of embedding and detection operations [12–14].

In this paper, it is hypothesized that when optimizing a large number of images of a same nature, it is possible to employ the knowledge acquired in previous optimization tasks in order to decrease the cost associated with frequent re-optimizations [19]. Knowledge of previous intelligent watermarking tasks has already been employed as a manner of improving subsequent tasks [20,21]. In such scenarios, the inherent optimization problems would share some similarity and intelligent watermarking can be cast as a single, long-term, *dynamic* optimization problem (DOP), instead of multiple, isolated, static problems. In a DOP, the optimum changes with time. Nickabadi et al. [22] observed that there are three different types of changes:

- Type I – Optimum location changes with time.
- Type II – Optimum fitness changes with time (but location remains fixed).
- Type III – Both, the location and fitness of the optimum change with time.

The authors also characterize a DOP according to change severity in both time (called *temporal severity*) and space (*spatial severity*). Yang and Yao [23] categorize environment changes in two groups: periodical, where changes occur in a fixed time interval and cyclical, where several fixed states occur repeatedly.

For an intelligent watermarking system, the moment an image transition occurs is known. Therefore, the temporal severity will be considered negligible, the problem is to be said pseudo-dynamic. More specifically, intelligent watermarking can be formulated as a specific type of DOP where a change is followed by a period of stasis [24]. In the envisioned scenario, an image transition should result in an environmental change. No change is expected to happen during the optimization of a single image. Thus, in the envisioned scenario, a stream of document images will correspond to a stream of optimization problems rather than a single problem where the optimum (or optima) continuously changes with time.

In this formulation of intelligent watermarking as a DOP, changes of type I are not expected as hardly two images will result in exactly the same fitness. Two images with very similar structure should result in a very similar set of optimal embedding parameters. That is, the set of embedding parameters can be either exactly the same or very similar, with only a small variation on their fitness values. The hypothesis we pose is that a transition between such similar images should result either in a change of type II (for the first case) or in a non-severe change of type III (for the second case). However, we will treat both as changes of type II. For the former, the location is exactly the same and it can be said that both optimal solutions are equivalent. For the later, the variation is still within the area surveyed by the population of solutions and thus there might exist other equivalent solutions that can be employed interchangeably for both problem instances. Two images with different structure by another way should result in considerable difference in both, set of optimal embedding parameters and respective fitness values. For this reason, a transition between them would imply in a severe change of type III. In such scenario, intelligent watermarking can be considered as a special case of cyclical problem [23] as similar rather than static states reappear over time.

For the scenario considered in this paper, embedding parameters will be optimized for a large stream of similar bi-tonal document images. For two similar images, $\mathbf{Co}_1$ and $\mathbf{Co}_2$, the change between the respective optimization problems would be of type II. The respective sets of optimal embedding parameters and fitness values are also expected to be similar. Since existing intelligent watermarking methods optimize embedding parameters for each image, computational time is wasted in optimizing parameters for a previously seen image. In such case, the population of solutions (sets of embedding parameters) obtained in the optimization of $\mathbf{Co}_1$ may have one or more solutions for $\mathbf{Co}_2$ that are comparable to those that would be obtained by performing complete re-optimization. Given two other images with considerably different structure, $\mathbf{Co}_3$ and $\mathbf{Co}_4$, the change would be of type III and re-optimization would be necessary as their respective optimal embedding parameters and fitness values are also expected to be very different. However, existing change detection methods do not provide means of measuring the similarity between two optimization problems which would allow re-using solutions for changes of type II.

In this paper, fast intelligent watermarking of streams of document images is formulated as a DOP and tackled with the use of a novel technique based on Dynamic PSO (DPSO) since canonical PSO cannot tackle some issues in a DOP like outdated memory, lack of a change detection mechanism and diversity loss [25,26]. In the proposed technique, solutions of previous problems are stored in a memory and recalled for similar problems. An adaptive technique to measure the similarity between optimization problems associated with two different images (change detection) is also proposed. This technique allows distinguishing between changes of types II and III. The main application of the proposed method is to tackle intelligent watermarking of long, homogeneous streams of document images. Both, this formulation of intelligent watermarking as a dynamic optimization problem and the adaptive change detection mechanism are unprecedented.

Proof-of-concept simulations are performed with the use of a general bi-tonal watermarking system based on odd–even embedding and quantization [4,27]. Two databases containing binarized pages of scientific documents were employed in these simulations. Simulation results demonstrate that this approach resulted in significant decrease in the computational cost of intelligent watermarking by avoiding costly optimization operations but with nearly the same accuracy of optimizing each image.

This paper is organized as follow. Section 2 presents a survey of digital watermarking and provides a baseline system for bi-tonal images. A baseline system for intelligent watermarking of isolated bi-tonal images based on PSO is presented in Section 3. The fast intelligent watermarking system based on DPSO is proposed in Section 4. Finally, Section 5 provides experimental results and discussions.

2. Digital watermarking methods for bi-tonal images

Since the intended application is the watermarking of document images (which is mostly based in bi-tonal encoding), a baseline bi-tonal watermarking method will be presented. Bi-tonal (or binary) watermarking offers additional challenges when compared to greyscale and color watermarking since in a bi-tonal image, pixels can only have two values – black or white – thus any variation tend to be more perceptible than in color and greyscale images. There are numerous bi-tonal watermarking techniques in the literature [4,27–35]. A survey of such techniques can be found in [36]. The main drawback of bi-tonal watermarking is that most techniques were conceived to deal with very specific applications like printed text, handwritten text, half-toned images or a certain class of watermarks (robust or fragile).

The bi-tonal method of Wu and Liu [4] is employed as the baseline watermarking method in this research since it is general and allows embedding multiple watermarks at the same image with different levels of robustness. This technique is based on odd/even embedding, where basically the image is partitioned into several

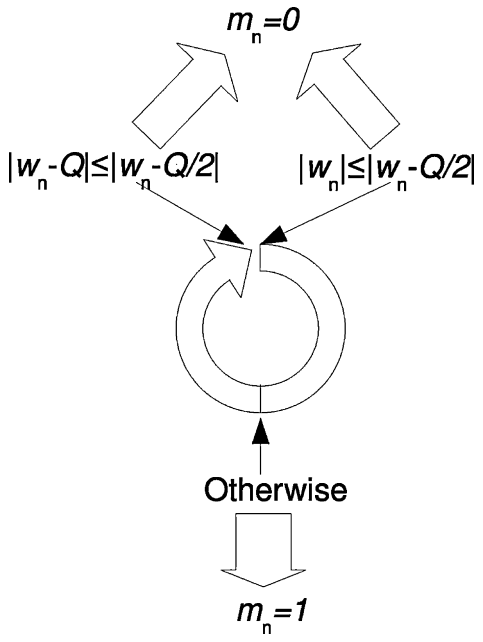

Fig. 1. Detection decision.

blocks of equal size ($B \times B$ pixels) and pixels are flipped in order to set the number of black pixels to either an odd number (to embed a '0') or an even number (to embed a '1'). The number of pixels to flip is quantized [37,38] as a manner of allowing robust watermarking. In this method, a bit m is embedded into the i th block of the cover image **Co** by manipulating the number of black pixels on that block (N_P) with the use of quantization

$$w_a = Q_\Delta\left\{N_P - Q\left(\frac{m}{2} + r\right)\right\} - \left(N_P - Q\left(\frac{m}{2} + r\right)\right) \quad (1)$$

where $Q_\Delta\{\}$ is the scalar uniform quantization operation, Q is the quantization step size and r is a pseudo-random number in the [0, 1) range. The new number of black pixels on block i (N'_P) is computed as

$$N'_P = N_P + w_a \quad (2)$$

Detection is performed by an inverse process. Image is partitioned using the same block size and a bit is detected from block i by verifying the number of black pixels on it (N''_P, which might be different than N'_P if image has been attacked)

$$w_n = Q_\Delta\{N''_P - rQ\} - (r - N''_P Q) \quad (3)$$

The detected bit m_n is set to 0 if the value of w_n is close to either 0 or Q. Otherwise (closer to $Q/2$), it is set to 1. This is depicted in Fig. 1. Basically, the value of w_n will be in the [0, Q] range and we have $|w_n| \leq |w_n - Q/2|$ when it is closer to 0 than to $Q/2$ and $|w_n - Q| \leq |w_n - Q/2|$ when it is closer to Q than to $Q/2$.

Flipping pixels in uniform areas results in visual artifacts. Flippability analysis techniques [4,27,31,34] tackle this problem by assigning a score to each pixel based on properties of its neighborhood. A window of size $W \times W$ is employed in this process. The look-up table (LUT) method proposed by Wu and Liu [4] uses a fixed 3×3 window in order to assign a score to a pixel based on the smoothness and connectivity of its neighborhood. A look-up table containing all the possible $2^{3\times3}$ patterns is built and the score for every pattern is calculated. For major window sizes, creating a look-up table becomes prohibitive.

Muharemagic [27] proposes a more flexible technique named Structural Neighborhood Distortion Measure (SNDM). This method uses a reciprocal distance matrix **D** in order to compute the flippability of a pixel, based on its $W \times W$ neighborhood. The SNDM of a candidate pixel (i, j) of image **Co** is computed as follows:

$$\mathbf{SNDM}_{i,j} = \frac{\sum_{k=-(W/2)}^{W/2}\sum_{l=-(W/2)}^{W/2}(\mathbf{Co}(i,j) \oplus \mathbf{Co}(i+k, j+l)) \times \mathbf{D}_{k+(W/2),l+(W/2)}}{\sum_{k=1}^{W}\sum_{l=1}^{W}\mathbf{D}_{k,l}} \quad (4)$$

where **D** is defined as:

$$\mathbf{D}_{i,j} = \begin{cases} 0, & \text{if}(i,j) = \dfrac{W}{2} \\ \dfrac{1}{\sqrt{(i-(W/2))^2 + (j-(W/2))^2}}, & \text{otherwise} \end{cases} \quad (5)$$

After that, pixels are shuffled using a pseudo-random sequence based on a seed S to in order to distribute flippable pixels evenly across the image. Muharemagic [27] observed that some seeds result in better (more uniform) shuffling than others for a given image. Thus, the use of a pool of shuffling seeds is preferred. After embedding, the image is de-shuffled. Detection consists of partitioning the image with the same block size used on embedding, shuffling all pixels (using the same key as well) and detecting the embedded bit on each block using the quantized detector. Flippability analysis is not necessary on detection as pixels do not need to be flipped. This watermarking process is explained in detail in [4] while an explanation of the SNDM technique can be found in [27].

Table 1
Range of embedding parameter values considered for PSO algorithm in this paper.

Embedding parameter	Particle encoding
Block size (B): {2, 3, 4, . . ., 62}	$x_{i,1}$: {1, 3, 4, . . ., 61}
Difference between Q for the robust (Q_R) and fragile (Q_F) watermarks (ΔQ): {2, 4, 6, . . ., 150}	$x_{i,2}$: {1, 2, .., 75}
SNDM window size (W): {3, 5, 7, 9}	$x_{i,3}$: {1, 2, 3, 4}
Shuffling seed index (S): {0, 1, 2, . . ., 15}	$x_{i,4}$: {0, 1, 2, . . ., 15}

3. Intelligent watermarking of isolated images using Particle Swarm Optimization (PSO)

Particle Swarm Optimization (PSO) [39] is an optimization technique inspired on the behavior of bird flocks. It relies on a population (swarm) of candidate solutions (particles). Each particle navigates in a multidimensional search space (or fitness landscape) guided by the best position visited by itself (cognitive component) and by its best neighbor (social component). A particle i has a position $\mathbf{x}_i$ and velocity $\mathbf{v}_i$ which are updated according to:

$$\mathbf{v}_i = \chi \times (\mathbf{v}_i + c_1 \times r_1 \times (\mathbf{p}_i - \mathbf{x}_i) + c_2 \times r_2 \times (\mathbf{p}_g - \mathbf{x}_i)) \quad (6)$$

$$\mathbf{x}_i = \mathbf{x}_i + \mathbf{v}_i \quad (7)$$

where χ is a constriction factor, chosen to ensure convergence [40], c_1 and c_2 are respectively the cognitive and social acceleration constants (they determine the magnitude of the random forces in the direction of $\mathbf{p}_i$ and $\mathbf{p}_g$ [39]), r_1 and r_2 are two different random numbers in the interval [0, 1], $\mathbf{p}_i$ is the best location visited by particle i and $\mathbf{p}_g$ is the best location visited by all neighbors of particle i. PSO parameters c_1 and c_2 are set to 2.05 while χ is set to 0.7298 as it has been demonstrated theoretically that these values guarantee convergence [39]. The neighborhood of a particle can be restricted to a limited number of particles (L-Best topology) or the whole swarm (G-Best topology). The particle encoding employed in this system can be seen in Table 1. Basically, the block size has lower bound of 2×2 and upper bound of 62×62 pixels (maximum possible for the given watermark size, considering the dimension of the images in the database). The remaining bounds, ΔQ, SNDM window size

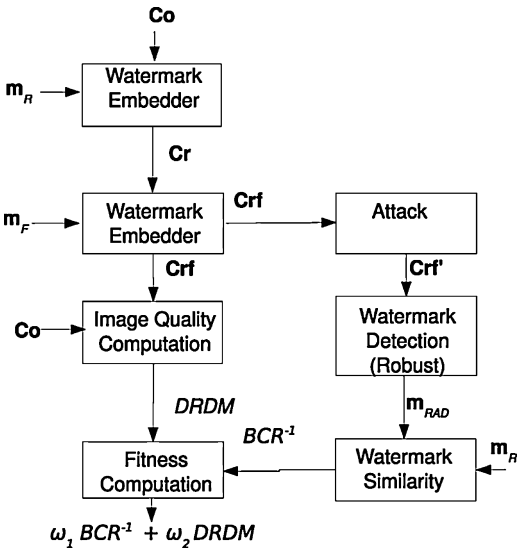

Fig. 2. Fitness evaluation.

and number of shuffling seeds were defined based on the literature [27].

Since one of the parameters in the intended application is a random shuffling seed (S) which leads to a multi-modal fitness landscape, L-Best topology will be employed in the proposed technique as it is known to outperform G-Best in such situation [41]. During initialization, each particle is set to communicate with its k-nearest neighbors (neighborhood is based on Euclidean distance). During optimization, the link between particles is changed in a random manner if no improvement occurs after one generation as a mean of improving adaptability [42]. Regarding the neighborhood size, we propose setting k to 3 as it is common found in the literature [43].

The application of PSO in the optimization of embedding parameters is straightforward. In the envisioned application, a population of potential solutions is initialized randomly according to the bounds defined in Table 1. Then, at each generation, the fitness of each particle $\mathbf{x}_i$ is evaluated in the task of watermarking a given image and $\mathbf{x}_i$ is adjusted according to Eq. 7. The fitness evaluation consists of embedding a robust and a fragile watermark – and is depicted in Fig. 2 where **Co** is the cover image, $\mathbf{m}_R$ and $\mathbf{m}_F$ are the robust and fragile watermarks, respectively, **Cr** is the robust watermarked image, **Crf** is the image that has been watermarked with both, the robust and the fragile watermarks (multi-level watermarked image), **Crf'** is the multi-level watermarked/attacked image, $\mathbf{m}_{RAD}$ is the robust watermark that has been detected from the multi-level watermarked/attacked image, DRDM is the Distance Reciprocal Distortion Measure, BCR^{-1} is the inverse of the Bit Correct Ratio [8,15] between $\mathbf{m}_R$ and $\mathbf{m}_{RAD}$, ω_1 is the weight assigned to BCR^{-1} and ω_2 is the weight assigned to DRDM.

The robust watermark is embedded first at a quantization step size Q_R and then, the fragile watermark is embedded at a quantization step size $Q_F < Q_R$. The robustness of the fragile watermark can be set to a fixed, small value (as it has to be destroyed in the event of an attack). For the robust watermark, the difference between both $\Delta Q = Q_R - Q_F$ will be optimized, with $Q_F = 2$. A secure channel is assumed to be available for the transmission of the optimal embedding parameters (Table 1).

Robustness is computed by embedding both watermarks, attacking the image, detecting the robust one and computing the inverse of the Bit Correct Ratio (BCR) [8,15] between the embedded and detected watermarks. As mentioned before, the fragile watermark does not need to be optimized and for this reason its robustness is not considered in the fitness evaluation. Quality is computed with the use of the Distance Reciprocal Distortion Measure (DRDM) [27] which is also based on the use of a reciprocal distance matrix with size $W \times W$. This limits the number of objective functions to two (which must be minimized). Both metrics are combined with the use of weighted aggregation [41]:

$$F(\mathbf{x}_i) = \omega_1 \text{BCR}^{-1} + \omega_2 \text{DRDM} \quad (8)$$

where ω_1 is the weight assigned to the robustness metric, BCR^{-1} is the robustness metric, ω_2 is the weight associated with the quality metric and DRDM is the quality metric. The weights are non-negative and $\omega_1 + \omega_2 = 1$.

More formally, a particle $\mathbf{x}_i$ represents a position in a 4-dimensional, discrete parameter space ($\mathbf{x}_i \in \mathbb{Z}^4$), with lower bound in (1, 1, 1, 0) and upper bound in (61, 75, 4, 15). This particle is mapped to a fitness function $F(\mathbf{x}_i)$ which consists of a weighted sum of the quality and robustness measurements obtained in a watermarking task involving the embedding parameters encoded by $\mathbf{x}_i$. The fitness landscape comprises the combination of both, parameter and fitness space.

4. Fast intelligent watermarking of image streams using Dynamic PSO

The proposed method assumes a long stream of bi-tonal document images ($\{\mathbf{Co}_1, \ldots, \mathbf{Co}_N\}$) and operates in two modes – a recall mode, where previously seen solutions are recalled from a memory and employed directly (avoiding re-optimization) and an optimization mode where the embedding parameters are optimized with the use of the L-Best PSO method described earlier until a certain stop criterion is met. Optimization will be halted whenever the global best has not improved for a given number of generations. The reason for choosing this criterion is that it is commonly found in the literature and it is not sensible to the number of generations chosen [44]. There are two levels of memory. The first one is named Short Term Memory (STM), which in our notation is represented by $\mathfrak{M}_S$ and contains all the particles obtained in the optimization of a single image, that is, the whole swarm. This set of particles will be called a **probe**. The second one is named Long Term Memory (LTM), represented by $\mathfrak{M}$ and contains probes obtained in the optimization of different images. Since optimization will only be triggered when images have different structure, given two probes $\mathfrak{M}_1$ and $\mathfrak{M}_2$, the solutions found in $\mathfrak{M}_1$ should be very distinct from the solutions found in $\mathfrak{M}_2$.

For each image, an attempt to recall the STM is made. If this recall is not successful, an attempt to the LTM is made. Change detection is employed during a recall in order to measure the similarity between the fitness landscape of current image and the fitness landscape of the image for which that probe was obtained. When STM/LTM recall fails, the best solutions from the STM probe are injected into the swarm replacing its worst solutions (those which resulted in poorest combination of quality and robustness) and optimization is triggered. Thus, the STM provides a first level of recall and memory-based immigrants for the swarm [45]. Regarding the amount of immigrant solutions, we propose injecting the best 70% particles, inspired by the results reported in [43], which employed the same amount of random rather than memory-based immigrant solutions.

This approach tackles diversity loss in a more precise manner than randomizing the entire swarm [45]. The proposed method is illustrated in Fig. 3. Here, starting with a first image ($\mathbf{Co}_1$), the swarm is initialized randomly (i) and optimization is performed until a stop criterion is attained, resulting in an optimized swarm (ii). A probe is created with the particles of the swarm obtained, put in the LTM (I) and copied to the STM (iia). After that (image

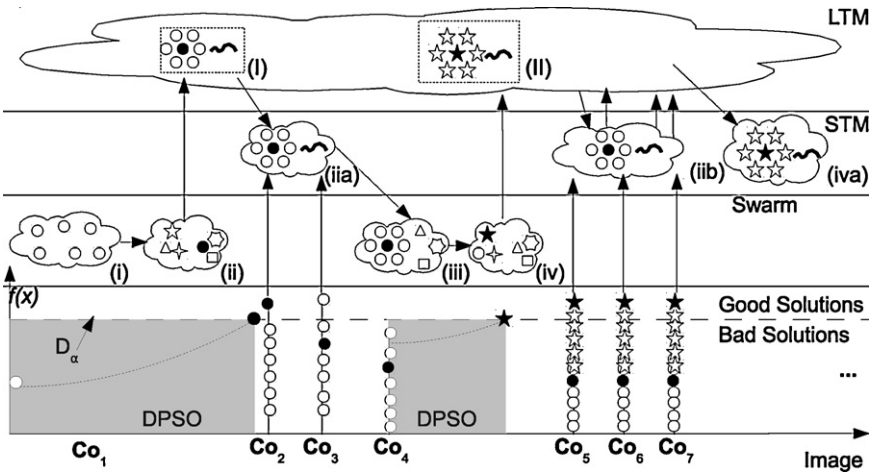

Fig. 3. Overview of the proposed method.

$\mathbf{Co}_2$), the global best is successfully recalled from the STM. A recall is successful whenever the difference between the distributions of fitness values of both probes is smaller than a critical value D_α. For image $\mathbf{Co}_3$ an alternative solution is recalled from the STM. Then, for image $\mathbf{Co}_4$, the STM recall fails and since the LTM probe is identical to the STM probe, the best solutions in the STM probe are injected into the swarm, replacing its worst solutions (iii). Optimization is triggered and results in another optimized swarm (iv). A second probe is created and put into the LTM (II). The probe in the LTM with the highest number of successful recalls (I) is copied to the STM (iib). Images $\mathbf{Co}_5$, $\mathbf{Co}_6$ and $\mathbf{Co}_7$ result in unsuccessful STM recalls. However, another LTM probe (II) is successfully recalled in both cases and its successful recall counter becomes greater than that of the current STM probe which is then replaced by it (iva).

During a transition between two images, the corresponding fitness landscape change can be either of type II (usually for images of a same nature) or III (images of different nature). It is possible to decrease computational burden by avoiding re-optimization for changes of type II – as for images $\mathbf{Co}_1$, $\mathbf{Co}_2$ and $\mathbf{Co}_3$ – since the optimum remains in the same location. Moreover, it is also possible to decrease computational burden of re-optimization for cases of type III by initializing the swarm with a few solutions from a previous optimization problem.

4.1. Change detection

The common strategy to perform change detection is to use fixed (sentry) particles (either from the swarm or from the memory [23,46]) and re-evaluate their fitness at each generation. However, such approach fails in detecting changes that occurred in restricted areas of the landscape as they are based on the assumption that if the optimum location of the fitness landscape changes, the fitness of any solution will also change [26]. The alternative is to choose one or more solutions randomly as sentries [26]. However, this approach does not allow measuring the severity of a change.

Wang et al. [47] try to tackle this problem by computing a running average of the fitness function for the best individuals over a certain number of generations, determining the severity based on a threshold. But this approach has two limitations in intelligent watermarking. The first is, it is not possible to put a threshold on variations of fitness value because of the issue regarding images with different capacity. The second is, since only the best solution is employed, it does not provide considerable information about the landscape.

Existing change detection methods use a limited number of sentries for a simple reason, they try to limit the number of fitness evaluations necessary in such process as in most of these cases, it needs to be performed at each generation. However, considering that in the envisioned scenario change detection will only be performed during image transitions, a larger number of sentries might be employed with little impact on the overall computational burden in cases where re-optimization is necessary and a significant decrease in cases where it is avoided. An intuitive approach is thus, use all particles as sentries. Considering that an appropriate diversity preserving mechanism is in place, such approach would provide more information about change in the fitness landscape than those based on single sentries. The L-Best topology employed in our technique maintains the diversity throughout the optimization process and should result in diverse enough probes. In the proposed change detection mechanism, the severity of a change between two images $\mathbf{Co}_i$ and $\mathbf{Co}_{i+1}$ is measured by evaluating the fitness value (Fig. 2) of a memory probe in both images and comparing the similarity between the respective distributions of fitness values with the use of a statistical test.

A slight difference between both distributions of fitness values might be due to change of type II or a non-severe change of type III. In such case, probe solutions could be employed directly, avoiding re-optimization. A severe difference between both distributions otherwise, can be due to a severe change of type III and re-optimization should be triggered. It is important to observe that the distinction between change types II and III is inferred indirectly as in a change of type III, the location of new optimum cannot be found with the use of sentries, requiring re-optimization for this end. However, in such situation, the severity of the variation for a given sentry is expected to be high, mainly if that sentry is positioned over a narrow peak. Since the distinction is based on the fitness distribution of sentry particles it is possible that two visually distinct images result in a similar distribution of fitness values. This means that although the images are different, their embedding capacity is equivalent and therefore, their optimal embedding parameters can be employed interchangeably.

Using a statistical test in the change detection process allows measuring the difference between the distributions of fitness values of a group of sentry particles in two different images. Such approach should provide much more information about a variation in the landscape than comparing fitness of isolated sentries. Fig. 4 illustrates this process for a slight variation in the landscape which might be due to a type II change in an hypothetical situation where the change in the landscape (due to an image transition) was completely symmetrical, that is probe 4 has now the same fitness value as probe 1 in the previous landscape and so forth. In such case, both distributions would be identical but the best solution

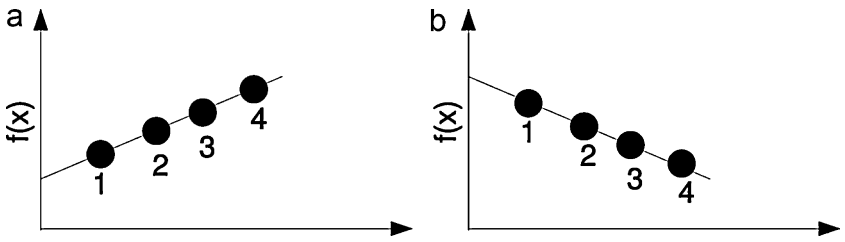

Fig. 4. Illustration of a perfectly symmetrical type II change. (a) Fitness values of sentry particles for first image. (b) Fitness values of sentry particles for second image.

Table 2
Values of c_α for confidence levels (two-sided) [49].

	Values					
Confidence level (α)	0.1	0.05	0.025	0.001	0.005	0.001
Coefficient (c_α)	1.22	1.36	1.48	1.63	1.73	1.95

for the first image (number 1) would not be the best for the next image. However, another solution (number 4) would be equivalent to previous best solution.

Fig. 5 illustrates the behavior of the change detection mechanism for a severe variation in the landscape, which might be due to a type III change. Here, both distributions differ significantly, no solution in probe could be employed directly in the second image.

Since the exact form of the fitness landscape is not known, no assumption can be made about the form of the distribution of fitness values of a probe. For this reason, the statistical test must be non-parametric. The Kolmogorov–Smirnov test (KS-test) [48] is a non-parametric statistical test that can be employed to compare the distribution of two sets of unidimensional points. It is based on the empirical distribution function (ECDF). Given a probe $\mathfrak{M}_i$, with L sentry particles $\{\mathfrak{M}_{i,1}, \ldots, \mathfrak{M}_{i,L}\}$ ordered according to their respective fitness values $\{f(\mathfrak{M}_{i,1}, \mathbf{Co}_i), \ldots, f(\mathfrak{M}_{i,L}, \mathbf{Co}_i)\}$ obtained in the optimization of image $\mathbf{Co}_i$, the empirical distribution function (ECDF) is defined as a set of cumulative probabilities $\{E_1, \ldots, E_L\}$:

$$E_j = \frac{n_j}{L} \tag{9}$$

where n_j is the number of fitness values less than $f(\mathfrak{M}_{i,j}, \mathbf{Co}_i)$.

Given two sets of fitness values obtained in the evaluation of a same probe in two distinct images $\{f(\mathfrak{M}_{i,1}, \mathbf{Co}_i), \ldots, f(\mathfrak{M}_{i,L}, \mathbf{Co}_i)\}$ and $\{f(\mathfrak{M}_{i,1}, \mathbf{Co}_{i+1}), \ldots, f(\mathfrak{M}_{i,L}, \mathbf{Co}_{i+1})\}$, the KS statistic gives the maximum distance between their ECDFs. The null hypothesis is that both sets of fitness values were drawn from the same distribution and it must be rejected if their KS statistic is above the critical value for a given confidence level (D_α). For large sample sizes (more than 12), the critical value can be computed as follows [49]:

$$D_\alpha = c_\alpha \sqrt{\frac{n_1 + n_2}{n_1 n_2}} \tag{10}$$

where n_1 is the number of elements in the first vector, n_2 is the number of elements in the second vector and c_α is the coefficient for confidence level α (Table 2).

4.2. A memory-based intelligent watermarking method using DPSO

The proposed method is depicted in Algorithm 1. Before optimization, STM and LTM will be empty (lines 2 and 3). For this reason, the swarm will be initialized randomly (line 4). Then, for each cover image ($\mathbf{Co}_i$), an attempt to recall the STM/LTM memory will be performed (line 7). If the recall fails, optimization is triggered and after that, the LTM memory ($\mathfrak{M}$) is updated with the swarm obtained in the end of the optimization process ($\mathfrak{S}_s$, lines 9 and 10).

Algorithm 1 *(Algorithmic description of the proposed method).*

Inputs:
$\mathbf{CO} = \{\mathbf{Co}_1, \ldots, \mathbf{Co}_N\}$ – set of cover images.
D_α – critical value for memory recall.

Definitions:
$\mathfrak{M}_S$ – Short Term Memory.
$\mathfrak{M}$ – Long Term Memory.
$\mathfrak{S}_s$ – set of solutions obtained in the optimization of $\mathbf{Co}_i$.
θ – recalled solution.
Recall($\mathbf{Co}_i, D_\alpha$) – recall STM/LTM memory (Algorithm 2).
Update($\mathbf{Co}_i, \mathfrak{S}_s, \mathfrak{M}$) – update STM/LTM memory (Algorithm 3).

1: {Initialization}
2: $\mathfrak{M}_S \leftarrow \varnothing$
3: $\mathfrak{M} \leftarrow \varnothing$
4: Initialize swarm randomly (respecting bounds defined in Table 1).
5: {Computation}
6: **for** $i \in [1, N]$
7: $\quad\theta \leftarrow Recall(\mathbf{Co}_i, D_\alpha)$
8: $\quad$**if** $\theta = \varnothing$
9: $\quad\quad$Optimize $\mathbf{Co}_i$ using PSO and watermark it using best solution $\mathbf{p}_g$.
10: $\quad\quad$*Update*($\mathbf{Co}_i, \mathfrak{S}_s, \mathfrak{M}$)
11: $\quad$**end if**
12: **end for**

After the first optimization, the STM will contain a single probe obtained at the end of the optimization of an image. Then, after at least two optimizations, the LTM will contain several probes, obtained at the end of the optimization of different images (more likely, images with little similarity among them). In practice, in situations involving long sequences of images with similar structure, the STM should allow a faster recall than the LTM. In the same scenario, the LTM should provide means of recalling solutions for images that do not resemble the majority of the images in an homogeneous database. Moreover, it should provide means of adapting to new homogeneous sequences of images being fed into the system.

The memory recall is summarized in Algorithm 2. During a STM recall, the probe ($\mathfrak{M}_S$) is re-evaluated for current image and a statistical test is employed to compare the similarity between both distributions of fitness values (line 3). If they are considered similar, the number of successful recalls of that probe ($Count_S$) is incremented (line 4) and the best solution is employed directly for current image, avoiding re-optimization (line 5). Otherwise, the LTM probes ($\{\mathfrak{M}_1, \ldots, \mathfrak{M}_L\}$) are sorted by their number of successful recalls ($Count_j$), in decreasing order (line 7) and the same procedure (fitness evaluation, followed by statistical test) is repeated for each probe until either a probe with similar fitness distribution is found or all probes have been tested (lines 9–13). After that, in both cases (successful or unsuccessful LTM recall), the probe with the highest number of successful recalls ($\max_{Count}(\mathfrak{M})$) is copied into the STM, replacing the previous one (line 15). If recall fails, the best STM solutions are injected into the swarm and re-optimization is triggered. There are two reasons for copying the LTM with highest number of successful recalls to the STM. The first is that for an homogeneous database, it should provide a better starting point in the event of re-optimization in comparison with re-randomization of the whole swarm. The second is that as the images in such scenario

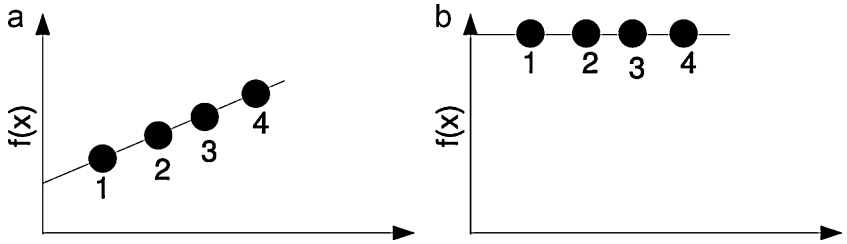

Fig. 5. Illustration of a type III change. (a) Fitness values of sentry particles for first image. (b) Fitness values of sentry particles for second image.

are expected to have a very similar structure, it makes sense trying to recall a probe that has been successfully recalled several times first.

Algorithm 2 *(Memory recall technique).*

Inputs:
$\mathbf{Co}_i$ – cover image i.
D_α – critical value for KS-test.

Outputs:
θ – optimal solution.

Definitions:
$\mathfrak{M}_S$ – Short Term Memory (one probe).
$\mathfrak{M}$ – Long Term Memory (set of probes).
L – number of LTM probes.
$Count_i$ – number of successful recalls for probe i.
$f(\mathfrak{M}_j, \mathbf{Co}_i)$ – evaluate probe $\mathfrak{M}_j$ in image $\mathbf{Co}_i$.
$KS(\mathbf{A}, \mathbf{B})$ – Kolmogorov-Smirnov statistic between vectors $\mathbf{A}$ and $\mathbf{B}$.

1: {Computation}
2: $\theta \leftarrow \varnothing$
3: **if** $KS(\mathfrak{M}_S, f(\mathfrak{M}_S, \mathbf{Co}_i)) \leq D_\alpha$**then**
4: $Count_S \leftarrow Count_S + 1$
5: Set θ with best solution in $f(\mathfrak{M}_S, \mathbf{Co}_i)$.
6: **else**
7: Sort $\mathfrak{M}$ by *Count* (in reverse order).
8: **for** $j \in [1, L]$
9: **if** $KS(\mathfrak{M}_j, f(\mathfrak{M}_j, \mathbf{Co}_i)) \leq D_\alpha$**then**
10: $Count_j \leftarrow Count_j + 1$
11: Set θ with best solution in $f(\mathfrak{M}_j, \mathbf{Co}_i)$.
12: Exit for.
13: **end if**
14: **end for**
15: $\mathfrak{M}_S \leftarrow max_{Count}(\mathfrak{M})$ /*Best probe is the first to be recalled and its best solutions are injected into the the swarm when re-optimization occurs.*/
16: **end if**

This is a direct memory scheme [50] since the global best and respective swarm solutions (probe) are kept in the memory. An unlimited memory is assumed at this moment, thus there is no need to delete any solution from the LTM. Each probe contains a set of solutions, their respective fitness values and the number of successful recalls for that probe.

The memory update is summarized in Algorithm 3. In the memory update mechanism, a new probe ($\mathfrak{S}_s$) comprising solutions obtained in the optimization of embedding parameters for an image ($\mathbf{Co}_i$), their respective fitness values and a successful recalls counter (initialized at 0, line 2) is added to the LTM (line 3).

Algorithm 3 *(Memory update technique).*

Inputs:
$\mathfrak{S}_s$ – set of solutions obtained in the optimization of $\mathbf{Co}_i$.
$\mathfrak{M}$ – Long Term Memory.

Definition:
$Count_L$ – success counter of new probe.

1: {Computation}
2: $Count_L \leftarrow 0$
3: Add $\mathfrak{S}_s$ to $\mathfrak{M}$.

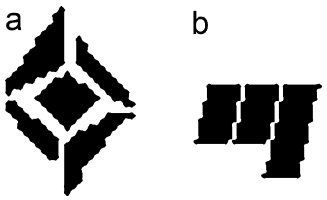

Fig. 6. Bi-tonal logos used as watermarks. (a) 26×36 BancTec logo. (b) 36×26 Université du Québec logo.

5. Experimental results

5.1. Methodology

In the following experiments, the swarm contains 20 particles, according to values found in the literature [39]. Optimization stops whenever no improvement in global best fitness occurs during 20 generations. This is considered quite conservative as literature suggests values between 5 and 20 [44]. In order to be able to compare the behavior of the proposed technique in different scenarios, full optimization will be applied to all images and the resulting optimal swarms will be employed in the experiments involving the memory-based technique. Since the fragile watermark must be destroyed in the case of tampering, Q_F will be fixed at 2. In such case, flipping a single pixel in one block changes the value of the embedded bit at that block. Full optimization will occur for every image in the experiments with isolated images using the PSO system and for every time a change is detected in the experiments using the memory-based DPSO system.

Three different experiments will be performed (A, B and C). In experiment A, the performance of the approach based on using full optimization (PSO) for each image is compared with that of a non-optimized set of parameters found in the literature [27]: $\{B=61,\ \Delta Q=8,\ W=3,\ S=0\}$. In experiment B, the performance of the proposed memory-based DPSO method is compared with that of the full optimization method. Finally, in experiment C, the memory-based approach is applied in a smaller dataset and then, the probes obtained in that dataset are provided as a sort of *a priori* knowledge in the optimization of a separate, larger dataset. In the memory-based experiments, the KS statistic, α was set to 0.05, which corresponds to a coefficient $c_\alpha = 1.36$ (Table 2) and a critical value (D_α) of 0.43.

The two watermarks to be embedded are the 26×36 BancTec logo (Fig. 6a) as robust watermark and a 36×26 Université du Québec logo (Fig. 6b) as fragile watermark.

Although most intelligent watermarking methods employ some kind of attack modeling [5] (i.e., apply an attack to watermarked images and measure the impact on robust watermark detection), the most simple scenario involves optimizing the parameters of the robust watermark against no attack. This is the approach to be followed in a first moment. Although it might seem trivial, it already requires choosing a set of parameters that makes the watermark robust enough to resist to the noise caused by the fragile watermark. Then, in a second moment, cropping attack (1% of image

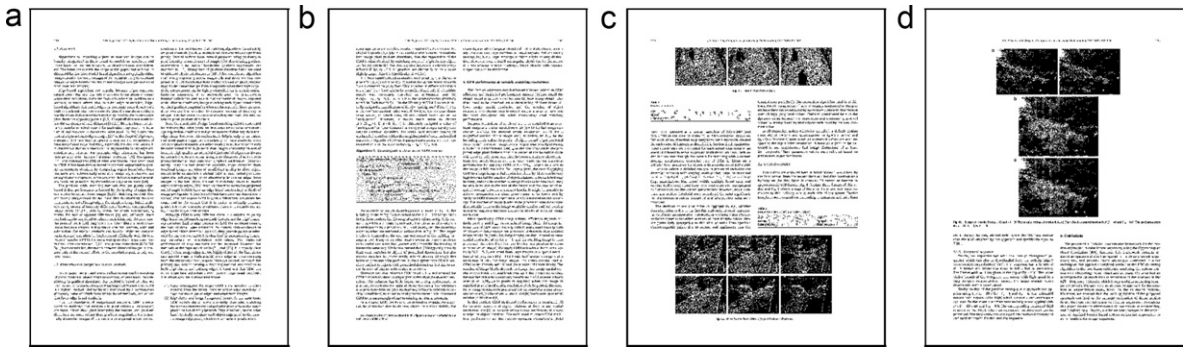

Fig. 7. Database samples. Each image has a density of 200 dpi and 1653 × 2206 pixels. (a and b) Text. (c and d) Half-toned image.

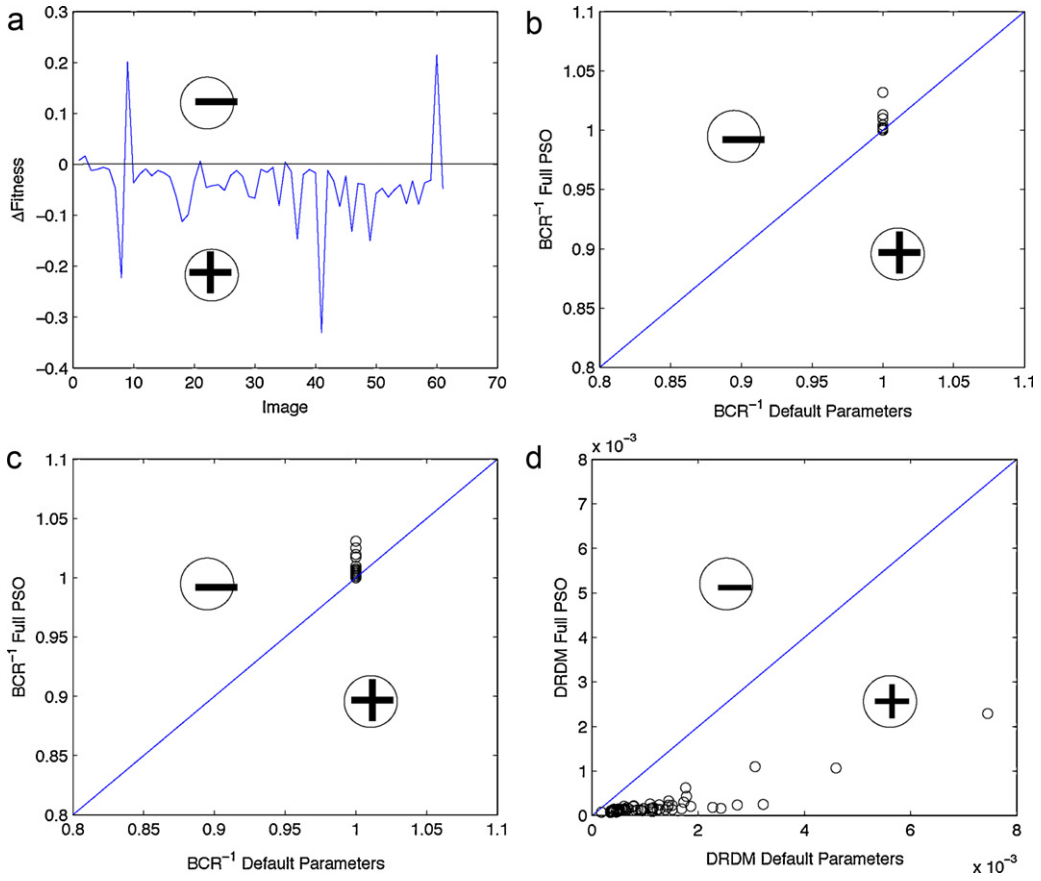

Fig. 8. Comparison of performance between optimized and non-optimized embedding parameters (TITI-61, without attack). The region below the diagonal line ('+') represents an improvement in performance by the PSO-based method. (a) Difference between fitness values. (b) BCR^{-1} robust watermark. (c) BCR^{-1} fragile watermark. (d) DRDM.

surface) will be employed. In both cases, the number of objective functions will be equal to two (which must be minimized) – visual distortion between cover and watermarked images (measured with the use of DRDM [27]) and the inverse of the watermark detection rate (in this case, inverse Bit Correct Ratio or BCR^{-1}) – according to Eq. 8. Since it was observed in the literature [27] that absolute value of optimal DRDM is significantly smaller than that of the optimal BCR^{-1}, the DRDM will be scaled by a factor of 10^2 (which should put them in a same magnitude). Finally, an equal weight will be employed in the aggregation technique ($\omega_1 = \omega_2 = 0.5$) since an equal trade-off between robustness and imperceptibility is sought.

5.1.1. Database

The first database consists of a stream of 61 pages of issues 113(1) and 113(2) of the Computer Vision and Image Understanding (CVIU) Journal. The stream was divided in four blocks, where the first and third contain 15 pages of plain text, the second and fourth contain 15 and 16 pages of text and half-toned images, respectively. This is the Text/Image/Text/Image (TITI-61) database. Fig. 7 shows some images from this database.

The second database contains 342 pages of 29 articles from CVIU 113(3) and 113(4) and will be named CVIU-113-3-4. These articles were converted to bi-tonal format with the use of

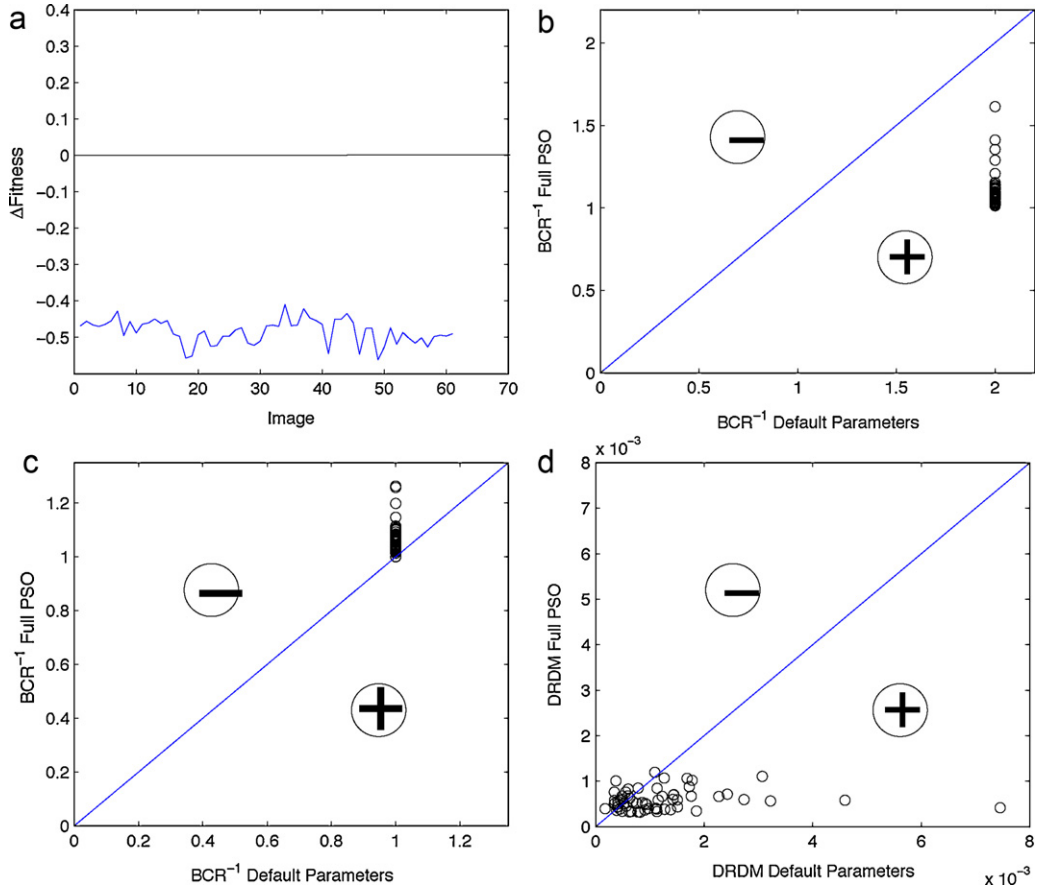

Fig. 9. Comparison of performance between optimized and non-optimized embedding parameters (TITI-61, cropping of 1%). The region below the diagonal line ('+') represents an improvement in performance by the PSO-based method. (a) Difference between fitness values. (b) BCR^{-1} robust watermark (after attack). (c) BCR^{-1} fragile watermark (before attack). (d) DRDM.

ImageMagick[1] convert utility at 200 dpi. The resulting images have 1653 × 2206 pixels. These two databases were chosen mainly because the articles are publicly available in the Internet and other researchers can download the images and set the same database using the same protocol employed in this article. Moreover, the resulting image streams are considerably homogeneous and some of the samples contain color images. This allows employing the same protocol in the event of adapting the proposed method to the optimization of color and/or greyscale watermarking systems.

5.2. A – Optimization of isolated bi-tonal images using full PSO versus default embedding parameters

The main purpose of the experiments performed is to compare the performance of the static PSO method with that of default embedding parameters found in the literature. A comparison of the fitness values obtained by PSO-based system with that obtained by employing the default parameters suggested in [27] shows that for most images, there was a decrease in fitness value. Fig. 8a provides such comparison for the TITI-61 database, without the use of attacks. In this figure, $\Delta Fitness$ means the fitness obtained by the use of optimized parameters less the fitness obtained by the use of default parameters. The impact of optimization on robustness was negligible (Fig. 8b). However, the use of optimization resulted in a significant improvement in the quality of the watermarked image (Fig. 8d) with negligible impact on the fragile watermark (the corresponding BCR is ≥95% for all cases as observed in Fig. 8c).

But the main advantage of optimizing embedding parameters is when it comes to making the robust watermark resistant against an attack. Fig. 9a shows $\Delta Fitness$ for the TITI-61 database, but with the use of cropping of 1%. In this particular case, such attack was employed during the optimization process (attack modeling). Regarding the default embedding parameters, they are the same as employed in Fig. 8. It is worth of notice that the optimized watermark is both more robust and less intrusive than the non-optimized robust watermark (Fig. 9b and d) with little impact on the fragile watermark (the corresponding BCR is ≥90% for most cases as observed in Fig. 9c).

Fig. 10 shows in detail the difference in terms robustness between the non-optimized and the optimized watermark. The cover image (Fig. 10a) is watermarked and then has 1% of its border cropped (Fig. 10b). A zoomed in view of a portion of the optimized watermarked image shows that indeed the impact on quality is minimal (Fig. 10c). For the non-optimized set of embedding parameters, both the robust and fragile watermarks were completely removed (Fig. 10d and e). However, for the optimized set of embedding parameters, the robust watermark resisted the attack (Fig. 10f) while the fragile watermark was completely removed (Fig. 10g). In this particular case, the set of optimal embedding parameters was $\{B=9, \Delta Q=16, W=3, S=4\}$ (it was $\{B=28, \Delta Q=4, W=3, S=11\}$ for the no attack modeling case).

[1] http://www.imagemagick.org.

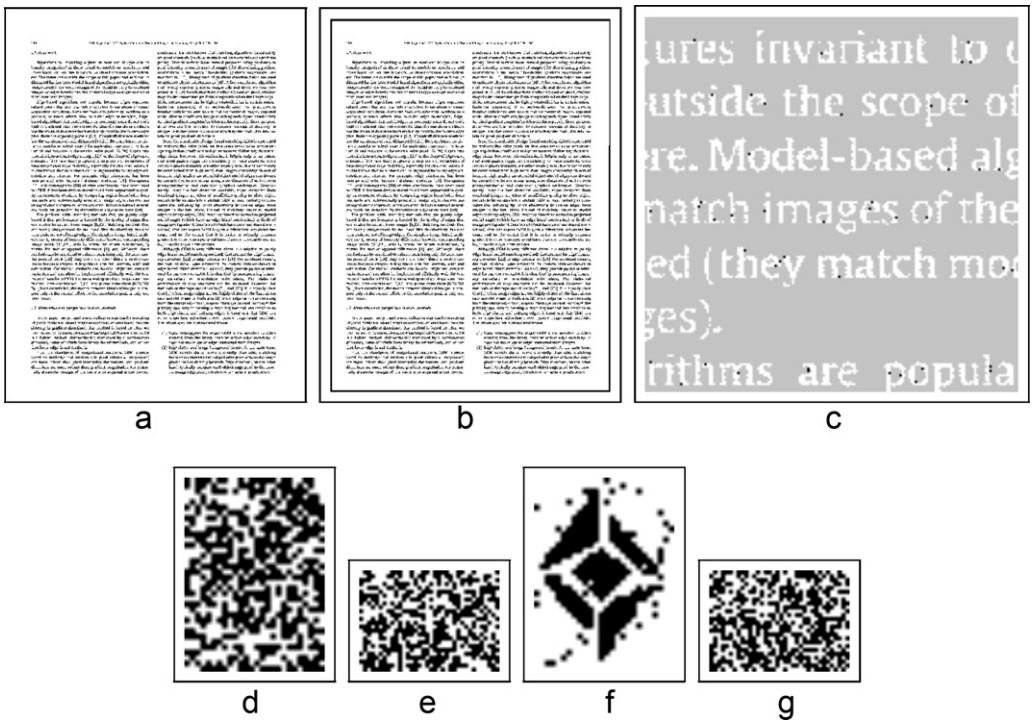

Fig. 10. Effect of optimizing embedding parameters on quality. (a) Cover image. (b) Cropped watermarked image. (c) Difference between optimized watermarked (against cropping of 1%) and original images. (d) Detected non-optimized robust watermark. (e) Detected non-optimized fragile watermark. (f) Detected optimized robust watermark. (g) Detected optimized fragile watermark.

This is the advantage of intelligent watermarking, it allows the optimization of embedding parameters for a specific attack (or set of attacks).

5.3. B – Optimization of streams of bi-tonal images using memory-based DPSO versus full PSO

The performance of the proposed method is compared with that of full optimization, in order to have a better understanding of the memory recall scheme (which is one of the main contributions of our method).

5.3.1. No attack

Fig. 11 shows the difference in fitness performance between the proposed method and full optimization ($\Delta Fitness$) for the TITI-61 database, without the use of any attack. It can be observed that this difference is negligible. It required 2760 fitness evaluations to optimize all 61 images with the proposed method against 51,460 fitness evaluations with full optimization (a gain of 94.6%). The Mean Squared Error (MSE) between the fitness values obtained by full optimization and by the proposed method is 5.4×10^{-6}. Full optimization was employed for image 1, resulting in a first probe which was put in the STM/LTM. Probe 1 was recalled from STM for images 2–7, 9–33, 35, 36, 38–40, 42, 43, 45–61. Re-optimization has occurred for image 8, resulting in probe 2, which was put into the LTM. Probe 2 was recalled from LTM for images 34, 37, 41 and 44.

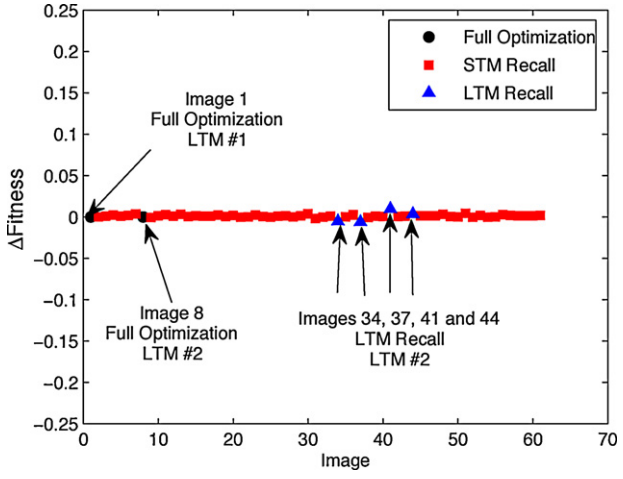

Fig. 11. Fitness performance of proposed IW algorithm for the 61 images of the TITI-61 database (without attack).

Regarding the two metrics that compose the fitness, the main variations were due to quality (DRDM). However, as it can be observed in Fig. 12, it was still quite similar to that of full optimization (MSE of 4.2×10^{-9}).

An interesting property of the memory scheme is that a probe also provides alternative solutions (other than the global best) during a recall. This can be observed in the histogram of recall of probe solutions (Fig. 13). It is possible to observe that for probe 1, the global best resulted in the best fitness 13 times while other probe solutions – 5, 6, 11 and 15 – resulted in the best fitness 24, 1, 7 and 10 times, respectively. For the other probes, the global best was recalled three times while another solution (14) was recalled once. What is worth of notice is that all STM recalls (probe 1) for images from the text category had either solutions 1, 5 or 11 as the best one (being the number of recalls 12, 4 and 7 respectively). And all STM recalls for images from the image/text category had either solutions 4 or 15 as the best one (with 20 and 10 recalls each, respectively). Thus, the same probe provided specialized solutions for different classes of images.

Another important observation is that all the STM recalls were made from the probe created by optimizing image 1 (which contains plain text and can be seen in Fig. 7a). Then, probe 2 was created by optimizing the parameters for text image but which contains a

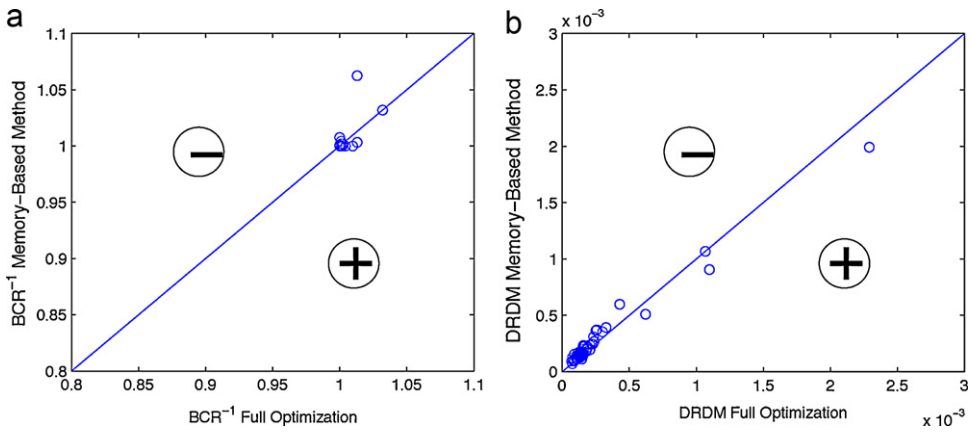

Fig. 12. Comparison of watermarking performance between full PSO and proposed method (TITI-61 database, without attack). The region below the diagonal line ('+') represents an improvement in performance by the memory-based method. (a) BCR^{-1} and (b) DRDM.

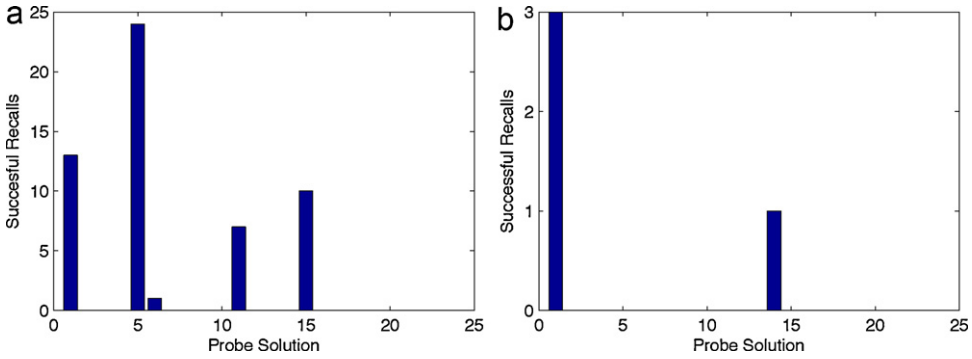

Fig. 13. Histogram of recall of probes 1 and 2 solutions (TITI-61 database, no attack). (a) Number of recalls of probe 1 solutions. (b) Number of recalls of probe 2 solutions.

significant blank space (Fig. 14a) and was recalled for other images with a significant amount of blank spaces (Fig. 14b–e). Thus, the main benefit of the proposed long term memory mechanism is to provide ready-to-use solutions for images with similar embedding capacity (mainly in cases involving images that are considerably different from the majority of the stream).

The behavior of the probes is analyzed more carefully for three specific cases. The first is a case of a successful STM recall (Fig. 15). Here, probe 1, which is based on image 1 is re-evaluated on image 2. It is possible to observe that both cumulative distributions are very similar, thus this is a change of type II and re-optimization was not considered necessary. Another interesting observation is that both cumulative distributions of fitness cover a significant range of fitness values, which allows comparing the similarity of both fitness landscapes more precisely than using isolated solutions. What is worth of notice in this case is that the best solution for image 2 was considered sub-optimal in image 1. That is, the probe provided an alternate solution in this case.

Fig. 16 shows a case of unsuccessful STM recall (Fig. 16a) followed by a successful LTM recall (Fig. 16b). In the first case, probe 1, which is based on image 1 is re-evaluated on image 37. Here, it is possible to observe that the distributions of fitness values in Fig. 16a are considerably different, which corresponds to a change of type III. What is worth of notice here is that images 1 (Fig. 7a) and 37 (Fig. 14c) are also quite different. However, probe 2, which is based on image 8 resulted in a very similar cumulative distribution of fitness value when re-evaluated on image 37, which corresponds to a change of type II (both images have a significant amount of blank spaces as it can be observed in Fig. 14a and c).

The same experiment was performed in the CVIU-113-3-4 database. Regarding the fitness, the performance was quite the same (Fig. 17).

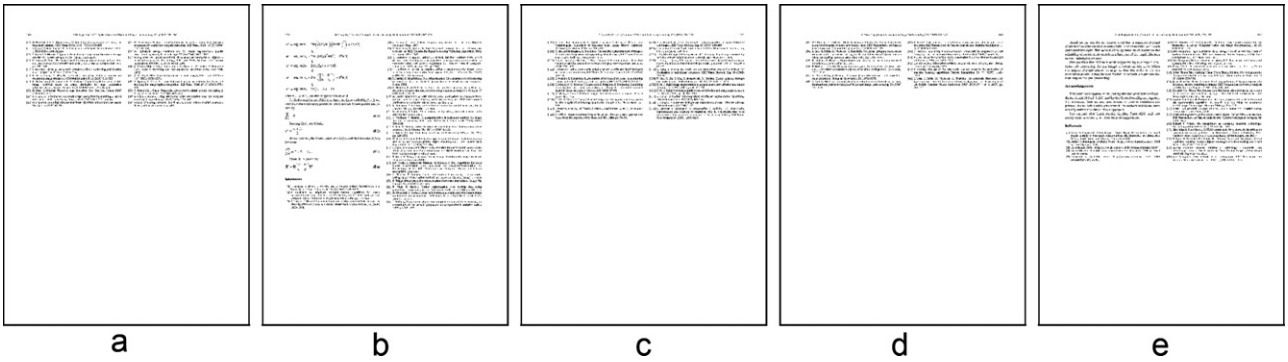

Fig. 14. Images that resulted in either re-optimization or LTM recall (probe 2). (a) Image 8. (b) Image 34. (c) Image 37. (d) Image 41. (e) Image 44.

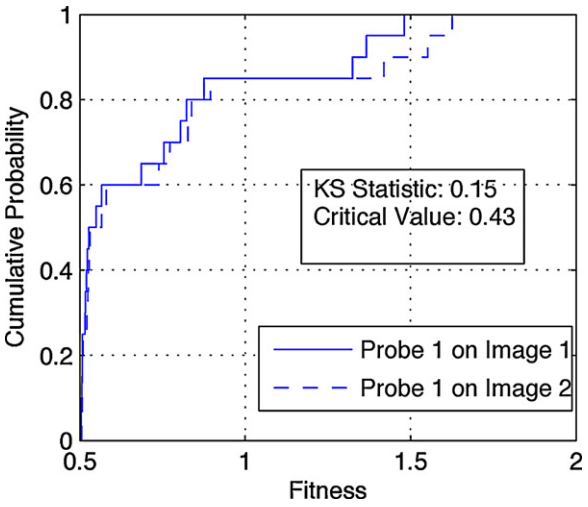

Fig. 15. Case of successful recall. Cumulative distribution of probe 1 on images 1 and 2.

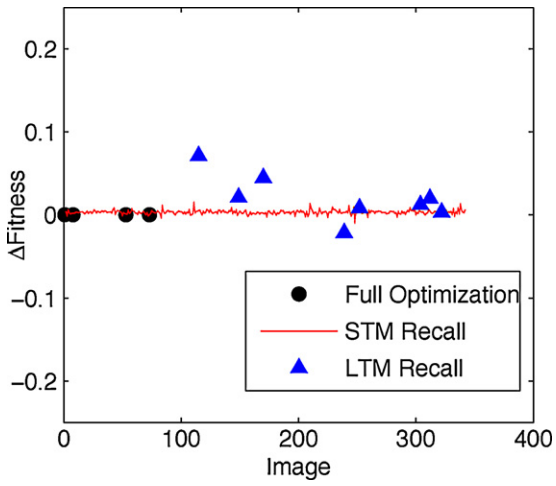

Fig. 17. Fitness performance of proposed intelligent watermarking algorithm for the CVIU-113-3-4 database.

The Mean Squared Error (MSE) between the two sets of 342 fitness values obtained by full optimization and the proposed method is 3.9×10^{-5}. The decrease in fitness evaluations was more significant (96.4%, which corresponds to 10720 fitness evaluations in the proposed method against 301580 in full optimization).

It is possible to observe that the behavior of the metrics that compose the fitness was very similar to what was observed for the TITI-61 database (Fig. 18).

Regarding the distribution of recalls per probe, for probe 1, the global best solution resulted in the best fitness evaluation for 315 recalls while another solution (20) was the best for 15 recalls. The 3 recalls of probe 2 were distributed among solutions 1 (global best), 11 and 20. The 5 recalls of probe 3 had solution 1 (global best) as the best one.

5.3.2. Attack modeling – cropping of 1% of image surface

The same experiments were performed using attack modeling (cropping of 1% of watermarked image area). The difference between fitness values can be seen in Fig. 19. Full optimization occurred twice (images 1 and 8). Probe 1 was employed in all STM recalls. As in the no attack case, the probe provided alternative solutions in numerous recalls (Fig. 20). For probe 2, solution 1 (global best) resulted in the best fitness five times while solution 2 was the best once.

It required 3960 fitness evaluations to optimize the 61 images against 55580 in full optimization mode (a gain of 92.9%). The MSE between both sets of fitness values was 1.4×10^{-4}. For the CVIU-113-3-4 database, although full optimization occurred twice, the gain in computational burden was a little bit higher (8740 fitness evaluations for the proposed method against 298100 for full optimization or 97.1%) for a MSE of 1.6×10^{-3}.

5.4. C – Optimization of streams of bi-tonal images using memory-based DPSO (learning mode) versus full PSO

In the first experiment involving learning, the probes obtained in the experiment with the TITI-61 database (no attack) were employed as a starting point for the CVIU-113-3-4 database (learning mode). Re-optimization was triggered twice and for this reason the number of fitness evaluations did not drop significantly when compared with the no-learning case. It required 10,560 fitness evaluations to optimize all the 342 images (a gain of 96.5% when compared with full optimization). The MSE was considerably smaller (2.3×10^{-5}) than without learning.

In the second one, solutions from TITI-61 (cropping of 1%) were employed as a starting point for the CVIU-113-3-4 database resulted in a slight improve in computational burden performance (a gain of 97.2% when compared with full optimization) as no full optimization was required. There was also a significant gain in precision (MSE of 2.1×10^{-4}).

Finally, to illustrate the cased-based learning capability of the proposed method, the images in the TITI-61 database (no attack) had their order shuffled and the same experiment was repeated for

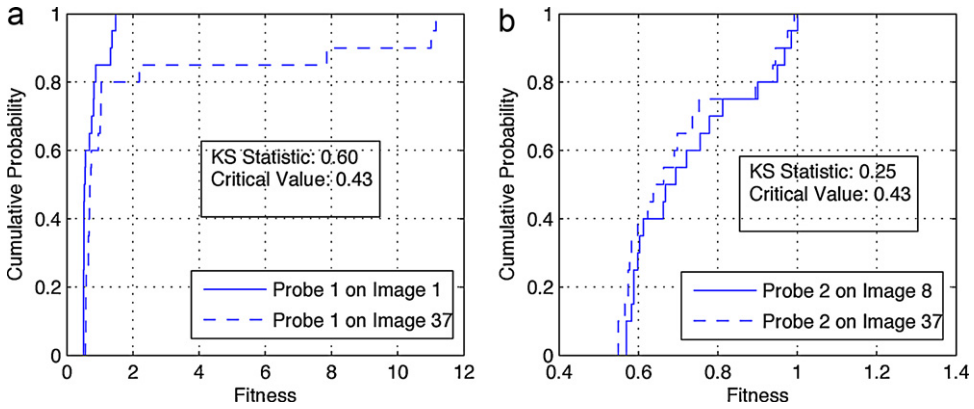

Fig. 16. A case of unsuccessful STM recall followed by a successful LTM recall. (a) Cumulative distribution of probe 1 on images 1 and 37 (unsuccessful STM recall). (b) Cumulative distribution of probe 2 on images 8 and 37 (successful LTM recall).

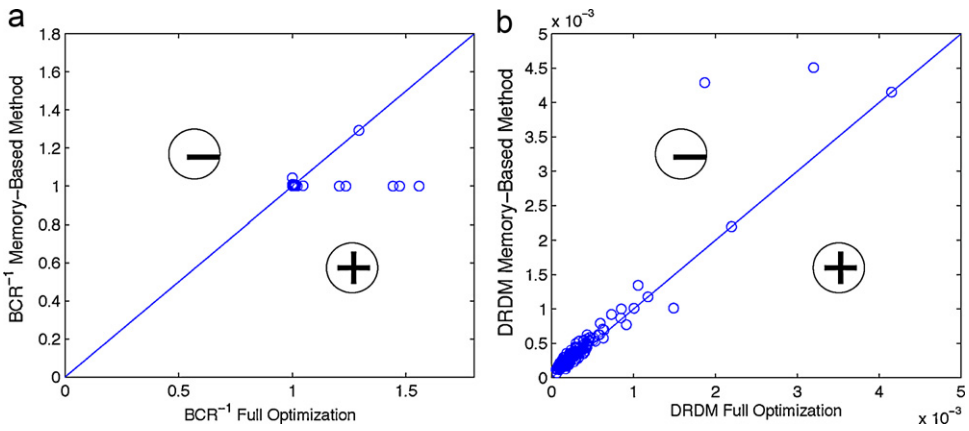

Fig. 18. Comparison of watermarking performance between Full PSO and proposed method (CVIU-113-3-4 database, without attack). The region below the diagonal line ('+') represents an improvement in performance by the memory-based method. (a) BCR^{-1} (b) DRDM.

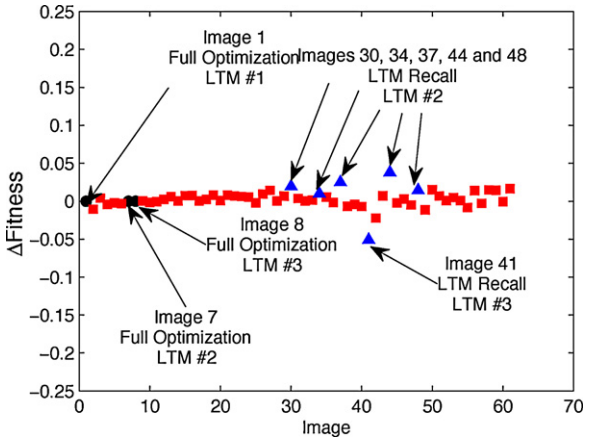

Fig. 19. Fitness performance of proposed IW algorithm for the 61 images of the TITI-61 database with cropping attack.

the same database, but using the memory from previous experiment as a starting point. This resulted in zero full optimization and exactly the same MSE.

5.5. Discussion

It was observed through the experiments involving the full PSO version of the proposed method and the default parameters that the optimization of embedding parameters is justified, mainly in situations involving adapting these parameters to a certain type of attack. In these experiments, it can be said that the trade-off between the watermark robustness and image quality are tailored to the specific need of a given scenario. That is, in situations where the only "attack" to be expected is the embedding of a second (fragile) watermark, the use of optimization resulted in an increase in the quality of the watermarked image when compared to default parameters. In situations involving an intentional attack, it was possible to obtain a watermark that is at the same time more robust and less intrusive. In both cases, it resulted in little or no impact in the robustness of the fragile watermark.

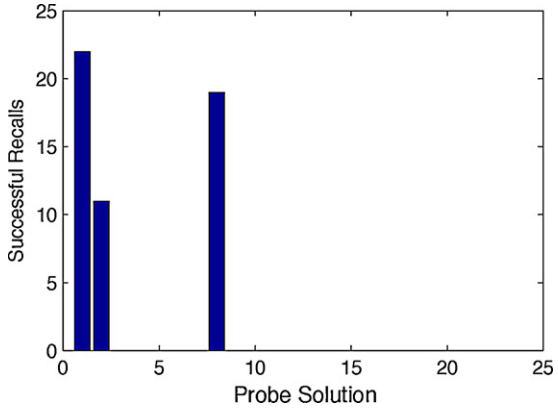

Fig. 20. Histogram of recall of probe 1 solutions (TITI-61 database with cropping attack).

Table 3
Simulation results.

Attack	Database	Learning	MSE full PSO vs. DPSO fitness	Decrease in fitness evaluations
No attack	TITI-61	No	5.4×10^{-6}	94.6%
No attack	CVIU-113-3-4	No	3.9×10^{-5}	96.4%
No attack	CVIU-113-3-4	Yes	2.3×10^{-5}	96.5%
Cropping 1%	TITI-61	No	1.4×10^{-4}	92.9%
Cropping 1%	CVIU-113-3-4	No	1.6×10^{-3}	97.1%
Cropping 1%	CVIU-113-3-4	Yes	2.1×10^{-4}	97.2%

In the experiments involving the memory-based approach, it was possible to observe that the proposed technique allowed a watermarking performance comparable to that of full optimization but for a fraction of the computational burden. Moreover, the memory provides a preliminary knowledge about a given intelligent watermarking task (learning capability).

The results are summarized in Table 3.

6. Conclusions

Since digital watermarking involves a trade-off between watermark robustness and image fidelity, numerous research papers have proposed the use of EC in order to find a setting of embedding parameters that result in an optimal trade-off for each specific image. However, this is a very costly process for high data rate applications as existing intelligent watermarking techniques rely on full optimization of embedding parameters for each image. This limits such approach to small proof-of-concept applications. In this paper, fast intelligent watermarking of streams of document images is formulated as a dynamic optimization problem and a novel intelligent watermarking technique based on Dynamic Particle Swarm Optimization (DPSO) is proposed. With this technique, solutions (i.e., embedding parameters) from previous optimizations are archived and re-considered prior to triggering new optimizations. In such

case, costly optimization were replaced by recall of previously computed solutions stored in memory. A practical application of the proposed technique would be the intelligent watermarking of massive amounts (e.g. tens of thousands per day) of different classes of documents like bank cheques, invoices and so on. The experimental results indicate that as long as different classes of images result in significant variation in the inherent fitness landscape of those images, the proposed technique should cope with those changes by triggering re-optimization. Moreover, in case of cyclical change, the memory should avoid costly re-optimization operations.

The proposed approach based on dynamic optimization is compared to the standard approach found in the literature which consists of applying full optimization to each image. To our knowledge, there is no approach based on dynamic optimization in the literature in order to make a comparison with the approach proposed in this paper. In general, the accuracy of the memory-based method is similar to that of a method based on full optimization but for a fraction of the computational cost. In situations involving homogeneous databases of document images, the use of the proposed memory-based DPSO resulted in gains of up to 97.2% in computational burden. The main reason is that for transitions involving images already optimized (which corresponds to a change of type II), the proposed method allowed recalling solutions from an archive directly, without need of re-optimization. It was also observed that the proposed adaptive change detection mechanism is robust enough to cope with minor variations in the fitness landscape between images with a similar structure (type II change) but is not discriminant enough to detect changes in the landscape between images with different structure (type III change). In addition, the proposed memory scheme provides a case-based reasoning capability to intelligent watermarking. A library of probes is incrementally built, which allows replacing costly full optimization operations by memory recalls. Such approach could be further improved by using statistical learning. This approach (as other intelligent watermarking approaches) assumes that a secure channel is available in order to make the optimal embedding parameters known at the detector.

In a future work, the performance of the proposed method will be analyzed in a more heterogeneous database. The performance is expected to be similar in a larger homogeneous database. However, an heterogeneous database should pose an additional challenge to the proposed technique. Since the main objective of this paper was formulating intelligent watermarking of an homogeneous stream of images, only one type of attack was employed in the objective function (cropping of 1%). This attack was chosen because it was observed in proof of concept experiments that merely cropping 1% of image surface resulted in severe loss for the robust watermark when default embedding parameters found in the literature were employed. Adding other attacks should make the problem more heterogeneous and will be addressed in a future work. Having different types of attacks for different images in the database should also make the problem more heterogeneous and thus, more challenging. The use of machine learning in order to create a probe based on properties of the fitness landscape will also be addressed. Comparison with other DPSO approaches was not considered in this paper because only one technique based on avoiding optimization for similar, cyclic problems was found in the literature [43] but this technique employs a change detection technique specific to the scenario addressed in that paper (pattern recognition). There are other promising EC techniques which could also be addressed in a future work like optimizing the heuristic parameters of PSO [41] and using Genetic Programming (GP) in order to develop a PSO algorithm tuned for a specific problem [51]. Finally, this framework should apply to different types of images and watermarking system since no property of the given system is employed during optimization other than robustness and quality (which are common to any watermarking system). The performance remains to be tested.

Acknowledgements

This work has been supported by National Sciences and Engineering Research Council of Canada and BancTec Canada Inc.

References

[1] I.J. Cox, J. Kilian, T. Leighton, T. Shamoon, A secure, robust watermark for multimedia, in: Workshop on Information Hiding, 1996, pp. 1–16.
[2] I. Cox, M. Miller, J. Bloom, Digital Watermarking, Morgan Kaufmann Publishers, 2002.
[3] M. Wu, Multimedia data hiding, Ph.D. thesis, Princeton University, 2001.
[4] M. Wu, B. Liu, Data hiding in binary image for authentication and annotation, IEEE Transactions on Multimedia 6 (4) (2004) 528–538.
[5] E. Vellasques, E. Granger, R. Sabourin, Intelligent watermarking systems: a survey, 4th ed., Handbook of Pattern Recognition and Computer Vision, World Scientific Review, 2010, pp. 687–724.
[6] J.H. Holland, Adaptation in Natural and Artificial Systems, MIT Press, Cambridge, MA, USA, 1992.
[7] J. Kennedy, R. Eberhart, Particle swarm optimization, in: Proceedings of IEEE International Conference on Neural Networks, Perth, Australia, 1995.
[8] T.E. Areef, H.S. Heniedy, O.M.O. Mansour, Optimal transform domain watermark embedding via genetic algorithms, in: Information and Communications Technology. ITI 3rd International Conference on Enabling Technologies for the New Knowledge Society, 5–6 December 2005, 2005, pp. 607–617.
[9] M. Arsalan, S.A. Malik, A. Khan, Intelligent threshold selection for reversible watermarking of medical images, in: Proceedings of the 12th Annual Conference Companion on Genetic and Evolutionary Computation, GECCO '10, ACM, 2010, pp. 1909–1914.
[10] C. Chen, C. Lin, A GA-based nearly optimal image authentication approach, International Journal of Innovative Computing, Information and Control 3 (3) (2007) 631–640.
[11] R. Ji, H. Yao, S. Liu, L. Wang, Genetic algorithm based optimal block mapping method for LSB substitution, International Conference on Intelligent Information Hiding and Multimedia Signal Processing (IIH-MSP'06). (December 2006) 215–218.
[12] P. Kumsawat, K.A. amd, A. Srikaew, A new approach for optimization in image watermarking by using genetic algorithms, IEEE Transactions on Signal Processing 53 (12) (2005) 4707–4719.
[13] C. Shieh, H. Huang, F. Wang, J. Pan, Genetic watermarking based on transform-domain techniques, Pattern Recognition 37 (3) (2004) 555–565.
[14] F.Y. Shih, Y. Wu, Enhancement of image watermark retrieval based on genetic algorithms, Journal of Visual Communication and Image Representation 16 (2) (2004) 115–133.
[15] J. Pan, H. Huang, L. Jain, Genetic watermarking on spatial domain, Intelligent Watermarking Techniques, World Scientific Co., 2004.
[16] Z. Wei, H. Li, J. Dai, S. Wang, Image watermarking based on genetic algorithm, IEEE International Conference on Multimedia and Expo. (July 2006) 1117–1120.
[17] Y. Wu, F.Y. Shih, Genetic algorithm based methodology for breaking the steganalytic systems, IEEE Transactions on Systems, Man, and Cybernetics, Part B 36 (February 1) (2006) 24–31.
[18] A. Khan, A.M. Mirza, Genetic perceptual shaping: utilizing cover image and conceivable attack information during watermark embedding, Information Fusion 8 (4) (2007) 354–365.
[19] T.M. Blackwell, P.J. Bentley, Dynamic search with charged swarms, in: GECCO '02: Proceedings of the Genetic and Evolutionary Computation Conference, Morgan Kaufmann Publishers Inc., San Francisco, CA, USA, 2002, pp. 19–26.
[20] A. Khan, S.F. Tahir, A. Majid, T. Choi, Machine learning based adaptive watermark decoding in view of anticipated attack, Pattern Recognition 41 (8) (2008) 2594–2610.
[21] I. Usman, A. Khan, Bch coding and intelligent watermark embedding: employing both frequency and strength selection, Applied Soft Computing 10 (1) (2010) 332–343.
[22] A. Nickabadi, M.M. Ebadzadeh, R. Safabakhsh, DNPSO: a dynamic niching particle swarm optimizer for multi-modal optimization, in: Evolutionary Computation. CEC 2008 (EEE World Congress on Computational Intelligence), 2008, pp. 26–32.
[23] S. Yang, X. Yao, Population-based incremental learning with associative memory for dynamic environments, IEEE Transactions on Evolutionary Computation 12 (5) (2008) 542–561.
[24] M. Farina, K. Deb, P. Amato, Dynamic multiobjective optimization problems: test cases, approximations, and applications, IEEE Transactions on Evolutionary Computation 8 (5) (2004) 425–442.
[25] T. Blackwell, Particle swarm optimization in dynamic environments, Evolutionary Computation in Dynamic Environments, Springer, 2007.
[26] A. Carlisle, G. Dozier, Tracking changing extrema with adaptive particle swarm optimizer, World Automation Congress, in: Proceedings of the 5th Biannual, vol. 13, 2002, pp. 265–270, doi:10.1109/WAC.2002.1049555.
[27] E. Muharemagic, Adaptive two-level watermarking for binary document images, Ph.D. thesis, Florida Atlantic University, December 2004.

[28] I. Awan, S.A.M. Gilani, S.A. Shah, Utilization of maximum data hiding capacity in object-based text document authentication, in: IIH-MSP '06: Proceedings of the 2006 International Conference on Intelligent Information Hiding and Multimedia, Washington, DC, USA, 2006, pp. 597–600.
[29] Q. Mei, E.K. Wong, N. Memon, Data hiding in binary text documents, in: SPIE Proceedings of Security and Watermarking of Multimedia Contents III, San Jose, USA, January 2001.
[30] H. Pan, Y. Chen, Y. Tseng, A secure data hiding scheme for two-color images, in: IEEE Symposium on Computers and Communication, 2000, pp. 750–755.
[31] A.T.S. Ho, N.B. Puhan, P. Marziliano, A. Makur, Y.L. Guan, Perception based binary image watermarking, in: 2004 IEEE International Symposium on Circuits and Systems (ISCAS), 2004, pp. 23–26.
[32] Y. Tseng, H. Pan, Secure and invisible data hiding in 2-color images, in: Twentieth Annual Joint Conference of the IEEE Computer and Communications Societies, vol. 2, 2001, pp. 887–896.
[33] H. Yang, A.C. Kot, Binary image authentication with tampering localization by embedding cryptographic signature and block identifier, Signal Processing Letters IEEE 13 (December 12) (2006) 741–744.
[34] C. Zhang, Z. Qiu, Fragile watermarking with quality control for binary images, in: Proceedings of the Fourth International Conference on Machine Learning and Cybernetics, 2005, pp. 4952–4956.
[35] J. Zhao, E. Koch, Embedding robust labels into images for copyright protection, in: International Congress on Intellectual Property Rights for Specialised Information, Knowledge and New Technologies, Vienna, Austria, 1995.
[36] M. Chen, E.K. Wong, N. Memon, S. Adam, Recent developments in document image watermarking and data hiding, in: Proceedings of SPIE 4518, 2001, pp. 166–176.
[37] B. Chen, G. Wornell, Quantization index modulation: a class of provably good methods for digital watermarking and information embedding, IEEE Transactions on Information Theory 47 (4) (2001) 1423–1443.
[38] J. Eggers, J. Su, B.B. Girod, Scalar costa scheme for information embedding, IEEE Transactions on Signal Processing 51(4) 2003.
[39] R. Poli, J. Kennedy, T. Blackwell, Particle swarm optimisation: an overview, Swarm Intelligence Journal 1 (1) (2007) 33–57, June.
[40] M. Blackwell, Particle swarms and population diversity, Soft Compututing 9(11) (2005) 793–802. http://dx.doi.org/10.1007/s00500-004-0420-5.
[41] K.E. Parsopoulos, M.N. Vrahatis, Recent approaches to global optimization problems through particle swarm optimization, Natural Computing: An International Journal 1 (2–3) (2002) 235–306.
[42] M. Clerc, Particle Swarm Optimization, ISTE Publishing Company, London, 2006.
[43] M.N. Kapp, R. Sabourin, P. Maupin, A PSO-based framework for dynamic SVM model selection, in: GECCO 2009, ACM, Montreal, Québec, Canada, 2009, pp. 1227–1234.
[44] K. Zielinski, R. Laur, Stopping criteria for a constrained single-objective particle swarm optimization algorithm, Informatica 31 (1) (2007) 51–59.
[45] J. Wang, Genetic particle swarm optimization based on estimation of distribution, Bio-Inspired Computational Intelligence and Applications. (2007) 287–296.
[46] J. Branke, Memory enhanced evolutionary algorithms for changing optimization problems, in: IEEE Congress on Evolutionary Computation CEC99, 1999, pp. 1875–1882.
[47] H. Wang, D. Wang, S. Yang, Triggered memory-based swarm optimization in dynamic environments, in: EvoWorkshops, 2007, pp. 637–646.
[48] NIST/SEMATECH e-Handbook of Statistical Methods, http://www.itl.nist.gov/div898/handbook/, March 2010.
[49] Critical values for the two-sample Kolmogorov–Smirnov test (2-sided), http://www.soest.hawaii.edu/wessel/courses/gg313/Critical_KS.pdf.
[50] S. Yang, Population-based incremental learning with memory scheme for changing environments, in: GECCO '05: Proceedings of the 2005 Conference on Genetic and Evolutionary Computation, ACM, New York, NY, USA, 2005, pp. 711–718. http://doi.acm.org/10.1145/1068009.1068128.
[51] A. Banks, J. Vincent, C. Anyakoha, A review of particle swarm optimization. Part ii: hybridisation, combinatorial, multicriteria and constrained optimization, and indicative applications, Natural Computing 7 (1) (2008) 109–124.